

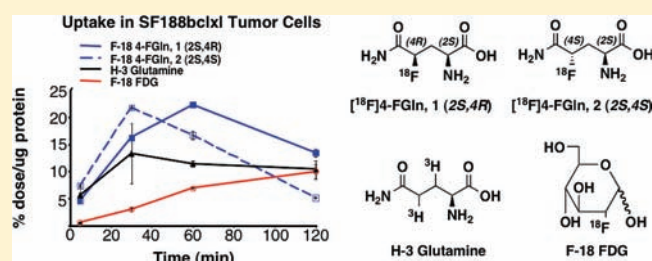
# Synthesis of Optically Pure 4-Fluoro-Glutamines as Potential Metabolic Imaging Agents for Tumors

Wenchao Qu,<sup>\*,†</sup> Zhihao Zha,<sup>†</sup> Karl Ploessl,<sup>†</sup> Brian P. Lieberman,<sup>†</sup> Lin Zhu,<sup>†</sup> David R. Wise,<sup>§,||</sup> Craig B. Thompson,<sup>§,||</sup> and Hank F. Kung<sup>\*,†,‡</sup>

Departments of <sup>†</sup>Radiology, <sup>‡</sup>Pharmacology, and <sup>§</sup>Cancer Biology, and <sup>||</sup>Abramson Cancer Centre, School of Medicine, University of Pennsylvania, Philadelphia, Pennsylvania 19104, United States

**S** Supporting Information

**ABSTRACT:** A versatile synthetic route to prepare all four stereoisomeric 4-fluoro-glutamines was developed by exploiting a Passerini three-component reaction. The skeleton of 4-substituted glutamine derivatives was efficiently constructed. Subsequent four-step reactions, highlighted by a “neutralized” TASF fluorination, provided the desired products with high yields and excellent optical purity. The optically pure fluorine-18 labeled 4-fluoroglutamines were also successfully prepared using either a 18-crown-6/KHCO<sub>3</sub> or K[222]/K<sub>2</sub>CO<sub>3</sub> catalysis system. Preliminary cell uptake and inhibition studies using the 9L tumor cells and SF188<sub>Bcl-xL</sub> tumor cells (a glutamine addicted tumor derived from glioblastoma) provided strong evidence for their potential application in conjunction with positron emission tomography (PET) for in vivo imaging of tumors, which use glutamine as an alternative energy source.



## INTRODUCTION

Amino acids (AAs) are essential chemicals for biological system. In addition to serving as the basic building blocks for peptides and proteins, they also perform various critical physiological functions as metabolic intermediates and neurotransmitters. Fluorine substituted AAs not only play important roles in peptide-based drugs and protein engineering,<sup>1–8</sup> but have also been particularly useful in positron emission tomography (PET) imaging for the diagnosis of cancer.<sup>9–14</sup>

It is now generally accepted that genetic alterations, such as the up-regulation of the PI3K/Akt/mTOR pathway (independent of hypoxia), can stimulate aerobic glycolysis and support tumor proliferation (Warburg effect). Recently, several reports have suggested that glutamine (Gln) can serve as an alternative source of metabolic energy for tumor cells.<sup>15–18</sup> Overexpression of the oncogene c-Myc (Myc) is essential for the coordinated expression of genes necessary for cells to use glutamine catabolism that exceed the cellular requirement for protein and nucleotide biosynthesis.<sup>19,20</sup> “Glutaminolysis,” especially in myc-overexpressing cells, plays a significant role in tumor growth and metabolism. This may represent an attractive new strategy for developing therapeutic and diagnostic agents for cancer therapy.<sup>18</sup> Therefore, Gln and its analogues may potentially be useful as metabolic indicators for studying the increased utilization of Gln in tumors. There is a significant interest in synthesizing all four stereospecific <sup>18</sup>F labeled 4-fluoro-glutamine (4-FGln) isomers: [<sup>18</sup>F]4-FGln, 1 (2S,4R); [<sup>18</sup>F]4-FGln, 2 (2S,4S); [<sup>18</sup>F]4-FGln, 3 (2R,4S), and [<sup>18</sup>F]4-FGln, 4 (2R,4R) (Figure 1) (Cautions: <sup>18</sup>F, T<sub>1/2</sub> = 110 min, 511 KeV, radioactive material). Among them,

1 and 2 are L-glutamine (natural amino acid) analogues, whereas 3 and 4 are D-glutamine (unnatural amino acid) analogues. They may serve as potential diagnostic tracers for positron emission tomography (PET) in order to assess glutamine utilization in various types of tumor cells (Figure 1).

To confirm the successful preparation and identity of these four <sup>18</sup>F labeled stereoisomers of 4-FGln (see Figure 1), a practical synthesis of the nonradioactive molecules is needed. Many reports on synthesizing various stereospecific fluorinated α-amino acids have appeared recently in the literature.<sup>21–37</sup> A review of synthetic methods for preparing 4-fluorinated glutamic acid and glutamine analogues was published by Dave et al. in 2003.<sup>38</sup> Preparation of diastereomeric mixtures of 4-FGln<sup>39</sup> was reported and <sup>18</sup>F labeled 4-FGln was also mentioned.<sup>40</sup> However, to the best of our knowledge, there is no specific report on the synthesis of optically pure 4-FGln and the <sup>18</sup>F labeled counterparts. The lack of literature reports on this topic is not surprising since there are formidable challenges facing the synthesis of such densely functionalized glutamine analogues. The presence of electron-withdrawing fluorine and carboxylic groups often induces undesirable epimerization at the C2 and C4 positions leading to the formation of four possible stereoisomers at different stages of preparation. Previously reported methods usually introduced a fluorine atom in an early stage of the whole synthesis, but we prefer a synthetic pathway that adds the fluorine atom at the very end (or as late as feasible) of the synthesis. Unlike a “normal” strategy for synthesizing fluorine substituted AAs,

Received: October 28, 2010

Published: December 29, 2010

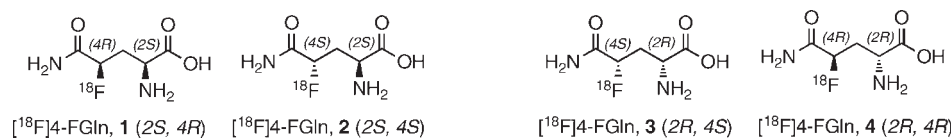


**Figure 1.** Structures of all four 4-fluoro-glutamine isomers:  $[\text{18F}]4\text{-FGln, 1 (2S,4R)}$ ;  $[\text{18F}]4\text{-FGln, 2 (2S,4S)}$ ;  $[\text{18F}]4\text{-FGln, 3 (2R,4S)}$ , and  $[\text{18F}]4\text{-FGln, 4 (2R,4R)}$ .

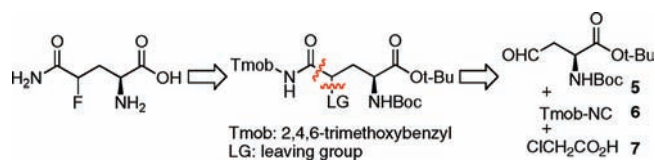


**Figure 2.** Retrosynthetic analysis for the preparation of 4-fluoro-L-glutamine via a Passerini three-component reaction.

the preparation of  $^{18}\text{F}$  labeled glutamine has to be simple and fast with a high yield incorporation of  $^{18}\text{F}$  very close to the final step, due to the short physical half-life of  $^{18}\text{F}$  ( $T_{1/2} = 110$  min). Such stringent requirements have placed additional obstacles beyond the problem of introducing a fluorine atom into a multifunctionalized glutamine backbone.

In this paper, we report the following: (1) stereospecific synthesis of 4-FGlns **1 (2S,4R)**, **2 (2S,4S)**, **3 (2R,4S)**, and **4 (2R,4R)** in a convergent manner; (2) analysis and confirmation of the structures of all 4-FGln stereoisomers; (3) development of practical methods for the preparation of all four isomers,  $[\text{18F}]4\text{-FGln, 1 (2S,4R)}$ ;  $[\text{18F}]4\text{-FGln, 2 (2S,4S)}$ ;  $[\text{18F}]4\text{-FGln, 3 (2R,4S)}$ , and  $[\text{18F}]4\text{-FGln, 4 (2R,4R)}$ ; (4) investigation of their ability to penetrate tumor cells as indicators of glutamine metabolism.

## RESULTS AND DISCUSSION

**Retrosynthetic Analysis and Intermediate Synthesis.** We hypothesized that the carbon-4 position functionalized glutamine skeleton could be assembled by aldehyde **5**, isocyanide **6**, and acid **7** via a Passerini three-component reaction (Figure 2)<sup>41,42</sup> This step also enabled the introduction of the amide protected with a 2,4,6-trimethoxybenzyl (Tmob) protecting group (PG). The Tmob group proved to be compatible in a “global” acidic deprotection condition at the end of the synthesis.<sup>43,44</sup> Initially, the other isocyanide, 2,4-dimethoxybenzyl (dmob) isocyanide, was introduced to form the dmob protecting group for the amide.<sup>45</sup> In the final deprotection stage, it was found that the removal of the dmob group by TFA was very sluggish.

Following our design, we first conducted the synthesis of two intermediates **5** and **6** (Scheme 1). Starting from a partially protected L-aspartic acid derivative **8**, esterification using *tert*-butyl trichloroacetimidate<sup>46</sup> under the catalysis of  $\text{BF}_3$  afforded the fully protected intermediate **9** with a 97% yield.<sup>47,48</sup> Removal of the benzyl group by catalytic hydrogenation followed by a mixed anhydride preparation and a subsequent sodium borohydride reduction gave homoserine **11** in 87% overall yield.<sup>49</sup> Subsequent oxidation of **11** with Dess-Martin periodinane (DMP)<sup>50</sup> provided aldehyde **5** in 86% yield.<sup>51,52</sup> The isocyanide **6** was prepared from 2,4,6-trimethoxybenzylamine **12**.<sup>43,44</sup> After conversion to formamide **13** by simply reacting with ethyl formate,<sup>53</sup> treatment with triphosgene gave **6** in 68% yield over two steps.<sup>54</sup>

Next, the Passerini three-component reaction was carried out. To our delight, the 4-acyloxy substituted Gln derivative **14** was successfully formed under mild reaction conditions in an efficient, atom-economical manner (95% yield). Simply treating **14** with

thiourea for selective removal of the chloroacetyl group resulted in a relatively low yield of the desired alcohol **15**.<sup>55</sup> Fortunately, adding a stoichiometric amount of  $\text{NaHCO}_3$  in this reaction dramatically improved the reaction yield to 91%.<sup>56</sup> The tosylation reaction of **15** gave tosylate **16** (the precursor for fluorination) in 96% yield (Scheme 2).

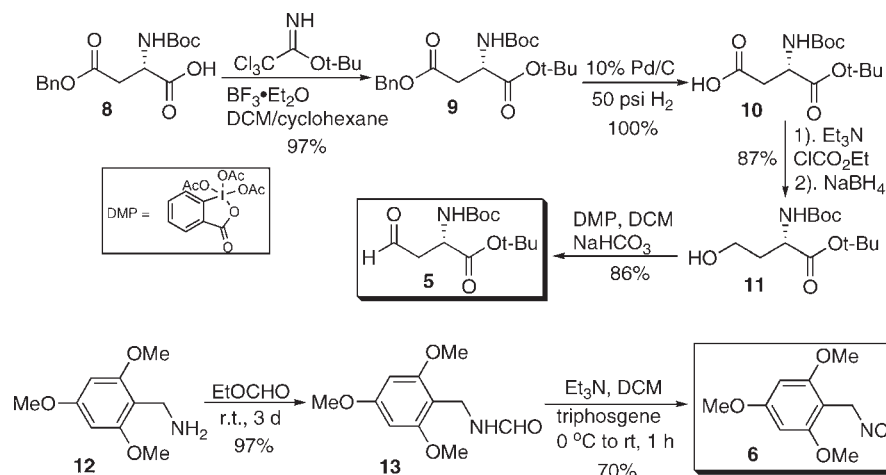
**Fluorination Reaction.** To explore the fluorination method leading to the desired fluorinated intermediate **19**, several precursors, **15–18**, were prepared and tested. The results of the fluorination reactions using different precursors and reagents are summarized in Table 1. Neither the reactions of alcohol **15** with (diethylamino)-sulfur trifluoride (DAST)<sup>57</sup> (entries 1 and 2) nor the reactions between tosylate **16** and potassium fluoride (KF) or tetrabutylammonium fluoride (TBAF) (entries 3–5) provided any desired product **19**.<sup>58</sup> Tetrabutylammonium difluorotriphenylsilicate (TBAT)<sup>59</sup> and tetrabutylammonium difluorotriphenyl stannate<sup>60</sup> (entries 6–8) gave only low yields despite a large excess of reagents used. As these approaches did not give satisfactory results, we investigated the use of the more active LG to replace the tosylate group. The preparation of triflate **17** by triflation of **15** was unsuccessful. The failure of this reaction may be due to the instability of this triflate. The preparation and separation of nosylate **18** was achieved later,<sup>61</sup> although a slow decomposition of **18** at room temperature was observed. Nevertheless, the reaction of TBAT with **18** did not afford any desired fluoride **19**.

Alternatively, a direct fluorination method (a combination of perfluoro-1-butanefluoride (PFSF)- $\text{NR}_3(\text{HF})_3\text{-NR}_3$  ( $\text{R} = \text{Et}$  or diisopropylethyl) with alcohol (**15**) reported by Yin was tested (entry 9).<sup>62</sup> Combinations of different bases ( $\text{Et}_3\text{N}$  or DIPEA), solvents (THF or MeCN), and substrate addition methods (one shot addition or slow addition via syringe pump) were tested but did not show any improvement (yield  $\leq 20\%$ ). Instead of the desired product, a large amount of intramolecular cyclized lactone **20** and the dimer **21** were produced in these reactions (Figure 3). A plausible explanation for this phenomenon is proposed in the Scheme 3. Interestingly, a similar phenomenon was also observed in the synthesis of (2S,4S)- and (2S,4R)-5-fluoroleucine.<sup>31</sup> Similarly, the bimolecular cyclization could be the reason for the formation of dimer **21**. Finally, the use of another hypervalent silicon fluorination agent, tris(dimethylamino) sulfonium difluorotrimethylsilicate (TASF), gave significantly improved yields (entry 10).<sup>63</sup> The yield was further improved (to 60–70%) (entry 11) by adding TASF in two portions at a 12-h interval.

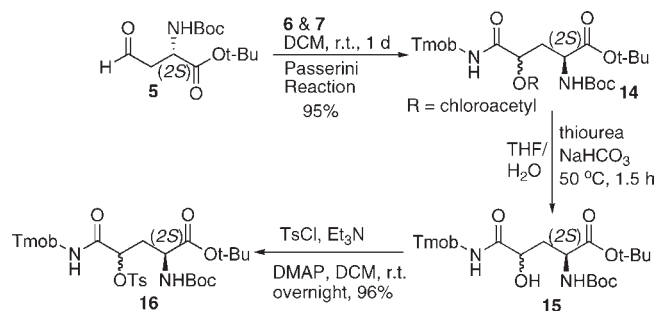
To our pleasant surprise, two diastereomeric 4-OH isomers of **15**, **22 (2S,4S)** and **23 (2S,4R)** (1:1 ratio based on HPLC analysis) could be separated by flash chromatography. The tosylation reaction provided **24 (2S,4S)** and **25 (2S,4R)** in excellent yields with no observed epimerization. Thus, the sequence of reactions provided ready access to the optically pure precursors for replacing 4-OTs with 4-F (Scheme 4).

**Optimization of the Fluorination Reaction and Synthesis of the Final Product.** After the exploration of the reactivity of TASF for the fluorination reaction, we turned our attention to

## Scheme 1. Synthesis of Intermediates 5 and 6



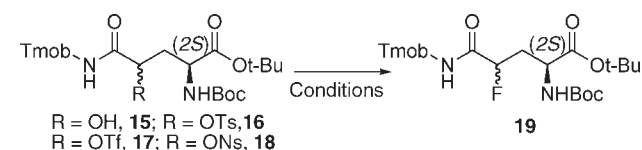
## Scheme 2. Synthesis of 4-Hydroxy and 4-Tosyl Substituted Gln



synthesizing two optically pure 4-FGLns, **1** (2*S*,4*R*) and **2** (2*S*,4*S*). Subsequent fluorination of **24** provided a 78% yield with a full inversion of stereochemistry at the C4-position and an epimerization at the C2-position (4-FGln derivative **26** (2*S*,4*R*) and **27** (2*R*,4*R*), 1:1 ratio) (Scheme 4). The TASF fluorination conditions selected above, which may be good enough for maintaining the S<sub>N</sub>2 fluorination reaction and fully invert the configuration at C4 position, did not maintain the stereospecificity at the C2 position. The basicity of the reagent TASF may be responsible for this observed epimerization at the C2 position.

We reasoned that moderating the basicity of the fluorination reagents might alleviate the above-mentioned epimerization. As reported previously, we employed a combination of TBAF and 2-mesitylenesulfonic acid to reduce epimerization at the C2 position in the synthesis of stereospecific 5-fluoroleucine.<sup>31</sup> Although directly following this method did not provide us with successful fluorination reactions, we returned to this idea with our agent, TASF. To reduce the basicity of TASF further, a milder acidic reagent Et<sub>3</sub>N·(HF)<sub>3</sub> was chosen. TASF was carefully titrated with Et<sub>3</sub>N·(HF)<sub>3</sub> to adjust the pH value of the reaction to 7–8. This “neutralized” TASF was tested for fluorination of the tosylate **24** (Scheme 5). After adding a more polar solvent (THF/CH<sub>2</sub>Cl<sub>2</sub> mixture) and increasing the reaction temperature, the conversion of the tosylate to fluoride **26** was achieved in a respectable yield (77%) with no epimerization at the C-2 position (Scheme 4). Using a slow evaporation

Table 1. Exploration Results of Fluorination Reaction



entry	conditions	substrate	yield (%) <sup>a</sup>
1	DAST, CH <sub>2</sub> Cl <sub>2</sub> , -78 °C to rt, 5 h	15	N/A
2	DAST, pyridine, toluene, rt 30 min to 80 °C 45 min	15	N/A
3	KF, TBAB <sup>b</sup> , DMF, 80 °C, 6 h	16	N/A
4	TBAF, THF, rt, 20 min	16	N/A
5	TBAF, MeI, THF, -78 °C to rt, 12 h	16	N/A
6	10–15 equiv TBAT, MeCN, 60 °C, 12–24 h	16	26–40
7	3 eq [Bu <sub>4</sub> N][Ph <sub>3</sub> SnF <sub>2</sub> ], MeCN, 60 °C, 24 h	16	19
8	10 equiv TBAT, MeCN, 60 °C, 3 h	18	N/A
9	PBSF, rt, Et <sub>3</sub> N/Et <sub>3</sub> N(HF) <sub>3</sub> or DIPEA/DIPEA(HF) <sub>3</sub> <sup>c</sup>	16	14–20
10	5 equiv TASF, CH <sub>2</sub> Cl <sub>2</sub> , 0 °C to rt, 12 h	16	40
11	2 equiv TASF, CH <sub>2</sub> Cl <sub>2</sub> , 0 °C to rt, 12 h, 2 more equiv TASF, 12 h at rt	16	60–70

<sup>a</sup> Isolated yields. <sup>b</sup> TBAB: tetrabutylammonium bromide. <sup>c</sup> MeCN or toluene as solvent, substrate was added with one portion or slow addition.

method, fine crystals of **26** were obtained and the structure was determined by X-ray crystallography (Figure 4), which assigned the absolute configuration of **26**. Finally, a global deprotection was accomplished by reacting the fully protected 4-FGln **26** with TFA/dimethyl sulfide (DMS) for 2.5 h.<sup>64</sup> Further purification using a Dowex 50WX8-200 (H<sup>+</sup> form) resin column, followed by recrystallization from EtOH/H<sub>2</sub>O, provided the final product, 4-FGln (2*S*,4*R*), **1**, in 71% yield.

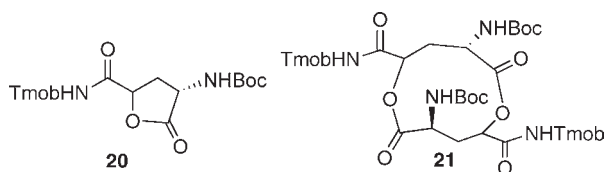
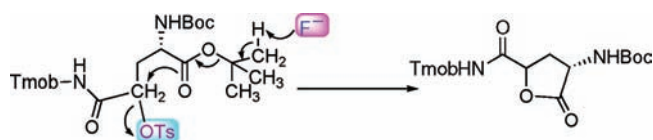


Figure 3. Structures of two byproduct in entry 9.

### Scheme 3. Plausible Mechanism for the Formation of Cyclized Byproducts 20 and 21



To determine the purity of the final product, a specific chiral HPLC method, which combines 1.0 mM  $\text{CuSO}_4$  aqueous solution as the mobile phase and reverse chiral column as the stationary phase with a control of column temperature (adjusted at 10 °C), was selected. This method clearly differentiated the four 4-FGln stereoisomers and the HPLC profiles demonstrated that the purity of 4-FGln **1** (2*S*,4*R*) was 98.8%. A slow evaporating recrystallization method provided excellent crystals of **1** and the X-ray crystallographic analysis (Figure 4) data further supported the structure assignment. The optically purified 4-FGln **1** (2*S*,4*R*) has never been presented before. The results reported in here firmly establish the configurations of each of the 4-FGln isomers, which will facilitate future applications of this series of biologically interesting and medically useful compounds.

We also accomplished the synthesis and assignment of 4-FGln **2** (2*S*,4*S*) (Scheme 5). Following the exact reaction conditions for synthesizing the fluoride intermediate **26**, the desired fluorinated glutamine derivative **28** was only obtained in 18% yield. By adjusting the pH value of TASF to 8–9, instead of 7–8 mentioned above, the fluorination yield reached 50%. However, under this higher pH condition, there was an increased epimerization byproduct **29** (ratio of **28**/**29**: 80/20), which made this reaction less attractive. After increasing the amount of “neutralized” TASF from 5 to 8 equiv, slightly decreasing the reaction temperature, as well as prolonging the reaction time from 10 to 24 h, the yield of this reaction was improved to 30%. Following the same deprotection and purification methods, the final product **2** was obtained in 67% yield. Chiral HPLC profiles showed that the purity of this product was 95%. Further attempts to recrystallize the product in order to remove a small amount of unwanted byproduct were not successful.

The different reactivity between tosylate **24** and **25** is not surprising. Krasnov and his colleagues investigated the nucleophilic substitution of two stereoisomers of 4-bromo substituted glutamate derivatives (Scheme 6).<sup>65,66</sup> First, they found that this type of reaction follows a “rigorous”  $\text{S}_{\text{N}}2$  mechanism, that is, a full inversion at the C4 position. Second, the bromide **31** (*erythro*) showed higher reactivity compared to the other stereoisomer, **30** (*threo*). The ratio of reaction rates ( $k_2$  to  $k_1$ ), *S*, ranges from 3 to 5 despite of the change of different solvents and different nucleophiles. They proposed a transition state model and concluded that the steric effect and the nonbonding interactions between the nucleophiles as well as the bulky functional groups of the

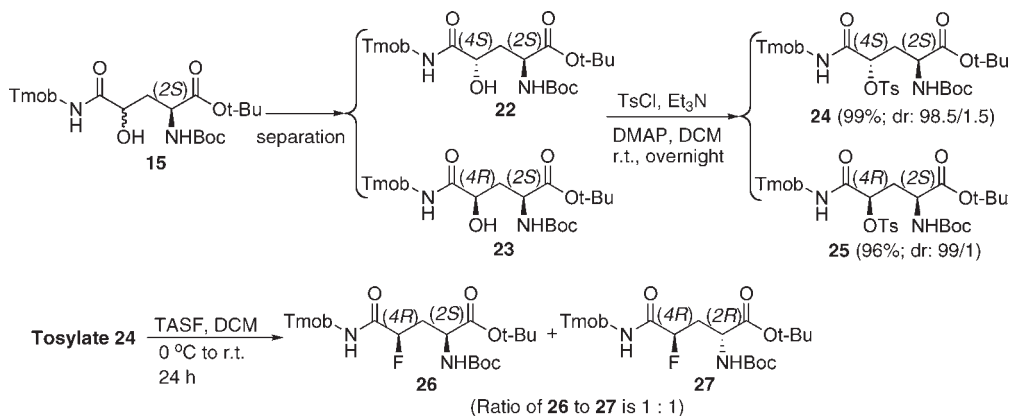
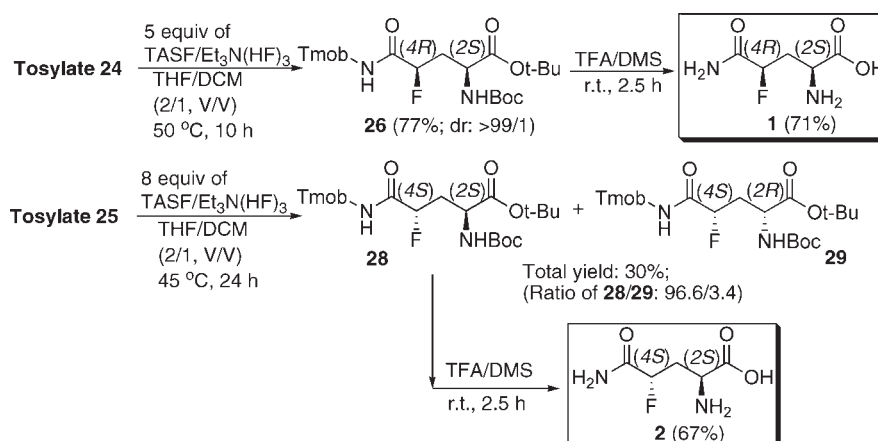
reactants contributed to the difference in reactivity. Interestingly, we observed an entirely reversed reactivity for the fluorination reaction. Tosylate **24**, a stereoisomer with a *threo*-configuration, showed better reactivity compared with *erythro*-tosylate **25**. In the case shown in Scheme 6, the relative bulky arylamine is the nucleophile whereas the small-sized bromide played the role of leaving group. In our example (Scheme 5), however, the size of the two groups is reversed. The nucleophile is a small fluoride and the bulky *para*-toluenesulfonyloxy group acts as the leaving group. Such a difference could account for the observed reactivity of the fluorination reaction in our study.

After successful synthesis of the desired 4-FGln products **1** and **2**, the other two 4-FGln stereoisomers, **3** and **4**, were also synthesized following the same synthetic strategy starting with partially protected unnatural D-aspartic acid **32** (Figure 5). The reaction yields and spectra of all of the D-isomer intermediates (**33**–**36**, **27**, and **29**) and the final products **3** (2*R*,4*S*) and **4** (2*R*,4*R*) were comparable with the analogue L-isomers with reversed optical rotation values. The X-ray crystal structures of fluoride **29** and 4-FGln **3** further confirmed the configuration assignments of these molecules (see Supporting Information).

**Development of Radiofluorination Methods.** To prepare the desired [ $^{18}\text{F}$ ]4-FGln at a “no-carrier-added” level, we tested a  $\text{S}_{\text{N}}2$  nucleophilic substitution reaction of “naked” [ $^{18}\text{F}$ ]fluoride with tosylate **16**, in the presence of Kryptofix 222 (K[222]) and  $\text{K}_2\text{CO}_3$  as the catalyst in  $\text{CH}_3\text{CN}$  at 80 °C for 10 min (the most commonly used  $^{18}\text{F}$  fluorination condition). It was found that, instead of [ $^{18}\text{F}$ ]26 and [ $^{18}\text{F}$ ]28, the two expected fluoride intermediates, all four possible isomers [ $^{18}\text{F}$ ]26–29 were formed in the reaction mixture (Scheme 7). While there was no starting material **16** left, a significant amount of elimination byproduct **37** was observed (determined by LCMS). The high basicity of both K[222] and  $\text{K}_2\text{CO}_3$  may be responsible for the epimerization at both of the C2 positions.

To avoid this epimerization during the  $^{18}\text{F}$  labeling reaction, a neutral phase transfer catalyst, tetrabutylammonium bicarbonate (TBABC), was tested as the radiolabeling catalyst. Surprisingly, similar to that observed for its fluorine-19 counterpart (Table 1, entries 3–5), the TBABC catalyzed reaction only afforded small amounts of labeled product using either  $\text{CH}_3\text{CN}$  or *tert*-butanol as the solvent.<sup>67</sup> Alternatively, a combination of a mild basic agent potassium bicarbonate ( $\text{KHCO}_3$ ) and a neutral phase transfer catalyst, 18-Crown-6, was tested for this “hot” labeling reaction. Using the tosylate precursor **24**, we found that the desired [ $^{18}\text{F}$ ]26, a (2*S*,4*R*) isomer, was successfully formed as the major product. Subsequently, the desired final product, [ $^{18}\text{F}$ ]1, was finally prepared by treating intermediate [ $^{18}\text{F}$ ]26 with TFA/anisole at 60 °C for 5 min (Scheme 7). A direct identification of [ $^{18}\text{F}$ ]1 can be performed successfully by coeluting it with 4-FGln **1** (2*S*,4*R*), a “cold” standard under the established chiral HPLC method. We were delighted to find that this method is also capable of separating and identifying all four radiolabeled and “cold” 4-FGln isomers **1**, **2**, **3**, and **4** (Figure 6). Upon the basis of this chiral HPLC analysis, we found that the  $\text{KHCO}_3$ /18-Crown-6 catalyzed radiolabeling method could prepare [ $^{18}\text{F}$ ]1 with high radiochemical and stereoisomeric purity (>95%).

Radiolabeling with [ $^{18}\text{F}$ ]fluoride starting from the four stereoisomeric precursors (**24**, **25**, **35**, and **36**) proved to be very tricky. As demonstrated above, the activation of [ $^{18}\text{F}$ ] fluoride by K[222] and  $\text{K}_2\text{CO}_3$ , a commonly used method to produce “naked” fluoride, readily led to epimerization. The basicity of K[222] and  $\text{K}_2\text{CO}_3$  promoted the epimerization of the C2 position (Scheme 7).

Scheme 4. Synthesis of Fluorination Precursors **24** and **25** as Well as Exploring Synthesis of Optically Pure 4-FGln **1**Scheme 5. Synthesis of Optically Pure 4-FGlns **1** and **2**

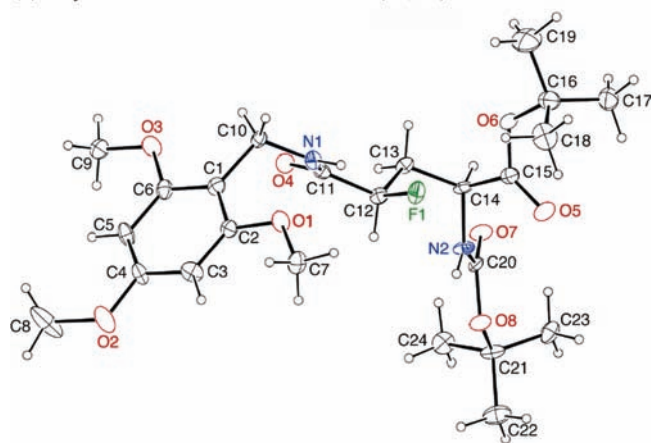
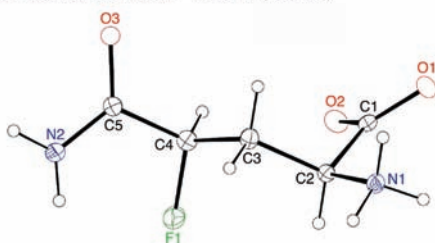
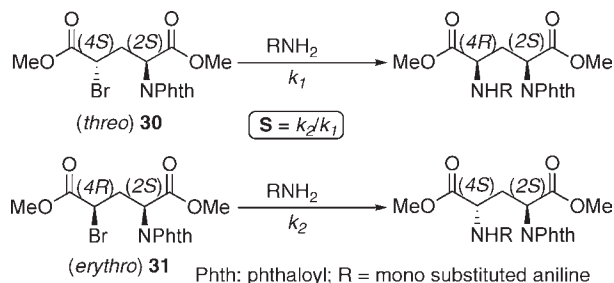
To circumvent the problem, a less basic catalyst system, 18-crown-6 and  $\text{KHCO}_3$ , was employed. The improved reaction conditions led to the successful conversion of two tosylate precursors **24** (2*S*,4*S*) and **35** (2*R*,4*R*) to the corresponding final products of [ $^{18}\text{F}$ ]4-FGln, [ $^{18}\text{F}$ ]1 (2*S*,4*R*), and [ $^{18}\text{F}$ ]3 (2*R*,4*S*), which contain only an inverted C4 position from that of the starting configuration. The starting precursors, **24** (2*S*,4*S*) and **35** (2*R*,4*R*) both have a similar *threo*-configuration for the 4-OTs and 2-NHBoc groups.

When the *threo*-configuration was switched to the *erythro*-configuration, such as for **25** (2*S*,4*R*) and **36** (2*R*,4*S*), the reactivity for  $^{18}\text{F}$  labeling changed significantly and unexpectedly (Scheme 8). Using 18-crown-6/ $\text{KHCO}_3$  as the catalysts for  $^{18}\text{F}$  fluorination of **25** (2*S*,4*R*) and **36** (2*R*,4*S*) led to the formation of [ $^{18}\text{F}$ ]4FGln, **3** (2*R*,4*S*) and [ $^{18}\text{F}$ ]4FGln, **1** (2*S*,4*R*) as the major products, respectively. It is important to note that the  $^{18}\text{F}$  fluorination reaction in the presence of 18-crown-6 and  $\text{KHCO}_3$  apparently inverted the C2 and C4 ( $\text{S}_{\text{N}}2$ ) positions simultaneously (double inversion). These findings are highly unexpected. Clearly, only the precursors with *erythro*-configuration yielded a “double-inversion” radiolabeling, that is, **25** (2*S*,4*R*) led to the formation of [ $^{18}\text{F}$ ]4FGln, **3** (2*R*,4*S*), while **36** (2*R*,4*S*) resulted in [ $^{18}\text{F}$ ]4FGln, **1** (2*S*,4*R*) (Scheme 8).

To obtain the two other stereoisomers of [ $^{18}\text{F}$ ]4-FGln, [ $^{18}\text{F}$ ]2 and [ $^{18}\text{F}$ ]4, an alternative process had to be pursued. When we conducted  $^{18}\text{F}$  fluorination of both *threo*-configuration precursors,

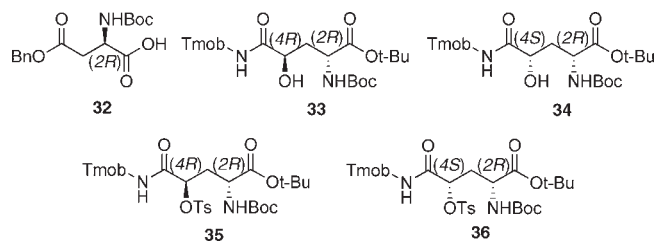
**24** (2*S*,4*S*) and **35** (2*R*,4*R*), under  $\text{K}[222]/\text{K}_2\text{CO}_3$  conditions, the results were more predictable. For precursor **24** (2*S*,4*S*), the labeling reaction led to a “predictable” and “repeatable” epimerization (1:1 ratio) at the C2 position and produced two final  $^{18}\text{F}$  labeled 4-FGlns, [ $^{18}\text{F}$ ]1 (2*S*,4*R*) and [ $^{18}\text{F}$ ]4 (2*R*,4*R*). Similarly, when precursor **35** (2*R*,4*R*) was treated with  $\text{K}[222]/\text{K}_2\text{CO}_3$  and [ $^{18}\text{F}$ ] fluoride, it led to the formation of [ $^{18}\text{F}$ ]2 (2*S*,4*S*) and [ $^{18}\text{F}$ ]3 (2*R*,4*S*) (1:1 ratio). To obtain each of the isomers selectively, the labeling intermediates containing all of the protecting groups were purified by HPLC and it was found that all of the isomers could be readily separated (Scheme 8 and Figure 7). Thus, all four isomers can be “predictably” prepared for further biological study.

One possible explanation for the above radio-fluorination results is presented in Scheme 9: tosylate precursors **25** and **35** can easily convert to each other under both reaction conditions (due to a base-induced epimerization at the C2 position). Because of the better reactivity of the *threo*-stereoisomer, **35**, compared with the *erythro*-isomer, **25**, the fluorinated product, [ $^{18}\text{F}$ ]29, can be formed in a faster manner relative to [ $^{18}\text{F}$ ]28 under both of the radiolabeling conditions. However, the further epimerization of the fluorinated product from [ $^{18}\text{F}$ ]29 to [ $^{18}\text{F}$ ]28 could not be promoted fast enough in a 15 min reaction period at  $70^\circ\text{C}$  under the 18-crown-6/ $\text{KHCO}_3$  conditions (a relative weak base). On the contrary, the  $\text{K}[222]/\text{K}_2\text{CO}_3$  (a stronger base) combined radiolabeling process could

(a). Crystal structure of intermediate **26** (2*S*,4*R*):(b). Crystal structure of final 4-FGln **1** (2*S*,4*R*):**Figure 4.** X-ray crystallography structures of **26** (a) and **1** (b), ORTEP drawing of the title compounds with 30% probability thermal ellipsoids.**Scheme 6. Nucleophilic Substitution of Bromide with Arylamine As Nucleophile: A Kinetics Study**<sup>65,66</sup>

convert [<sup>18</sup>F]**29** to [<sup>18</sup>F]**28** fast enough to form a roughly 1:1 mixture of [<sup>18</sup>F]**29** and [<sup>18</sup>F]**28** (Figure 7) after a 10 min reaction period at 80 °C.

There are several challenging issues associated with the preparation of <sup>18</sup>F labeled 4-fluoroglutamine. First, there are two optical centers (the C2 and the C4 positions) in this molecule that can, theoretically, lead to the possible formation of four stereoisomers (**1**, **2**, **3**, and **4**) during the synthetic process. Second, the α-amino group is adjacent to the carboxylic acid, and therefore, as in other naturally occurring α-amino acids, it is easily epimerized under basic conditions. Next, the glutamine contains a labile amide group, which can easily hydrolyze to form glutamic acid. The glutamine and also glutamic acid are readily converted, or cyclized, to form pyroglutamic acid under either acidic or basic conditions. As such, 4-fluoropyroglutamic acid is a common impurity in the preparation of 4-FGln. In addition, when the 4-FGln derivatives are synthesized by the S<sub>N</sub>2 fluorination reaction, it often produces the elimination byproduct,

**Figure 5.** Structures of starting material D-aspartic acid derivative **32** and two sets of intermediates **33** and **34**, **35** and **36**.

especially during the preparation of [<sup>18</sup>F]4-FGln. To avoid this side reaction, a careful control of the reaction temperature and basicity is essential. The methods described in this paper for the synthesis of stereoisomers of “hot” and “cold” 4-FGln put forward a relatively simple strategy to obtain these otherwise hard to produce isomers. Although further improvement of the radiolabeling yield may be necessary, it is apparent that the *threo*-precursor, **24**, can be directly radiolabeled under 18-crown-6/KHCO<sub>3</sub> conditions to give the desired L-glutamine isomer [<sup>18</sup>F]4-FGln, **1** (2*S*,4*R*) as a major product.

**Biological Evaluation of [<sup>18</sup>F]4-FGln ([<sup>18</sup>F]**1**, [<sup>18</sup>F]**2**, [<sup>18</sup>F]**3**, and [<sup>18</sup>F]**4**).** The cell uptake of the four [<sup>18</sup>F]4-FGln isomers was evaluated using the 9L and SF-188 tumor cell lines. The cell uptake results (% dose/100 μg protein) were compared to those of [<sup>3</sup>H]-L-glutamine. The 9L tumor cells are commonly used for studying tumor metabolism and amino acid uptake.<sup>10,68,69</sup> The transformed SF188-Bcl-x<sub>L</sub> tumor cells with up-regulation of c-myc gene were reported to have a significant “addiction” to the L-glutamine;<sup>15,16</sup> therefore, they were also used to test the hypothesis that the new [<sup>18</sup>F]4-FGln isomers are suitable glutamine mimetics for imaging the “glutaminolysis” in tumor cells.

There were distinctive differences among all the isomers (Figure 8); while [<sup>18</sup>F]FDG displayed the expected high uptake and retention in the 9L cells. The two isomers with 2*S* configuration, the natural L-amino acid of Gln derivatives, displayed the highest uptake. The [<sup>18</sup>F]4-FGln, **1** (2*S*,4*R*), showed a high uptake in 9L cells and the uptake continued nonstop for 2 h, the maximum time point studied. The [<sup>18</sup>F]4-FGln, **2** (2*S*,4*S*), also displayed excellent uptake similar to that of **1** (2*S*,4*R*). However, it appeared that the uptake value dropped precipitously at 2 h (Figure 8). The mechanisms responsible for the efflux at this later time point are unclear at this stage. The unnatural D-Gln (containing the D-amino acid), [<sup>18</sup>F]4-FGln isomers, **3** (2*R*,4*S*), and **4** (2*R*,4*R*), all showed a drastically lower cell uptake as compared to the [<sup>18</sup>F]4-FGln, **1** (2*S*,4*R*), and **2** (2*S*,4*S*), as well as the [<sup>3</sup>H]-L-Gln, suggesting that the configuration of the amino group at the C-2 position is critical for tumor cell uptake, and that the 2*S* configuration of Gln (commonly known as the L-isomer) is essential for transportation across the cell membrane.

The tumor cell uptake of [<sup>18</sup>F]4-FGln is a highly selective process; the two <sup>18</sup>F labeled native L-Glns (2*S*) displayed a higher uptake than that of the <sup>18</sup>F labeled unnatural D-Glns (2*R*). It is likely that the [<sup>18</sup>F]4-FGln, **1** (2*S*,4*R*), and [<sup>18</sup>F]4-FGln, **2** (2*S*,4*S*), enter tumor cells through an active transport system. Once inside the cells, just as in the case of naturally occurred L-Gln (2*S*), the glutaminase may strip off the amino group at the C5 position. Subsequently the C2 amino group would also be removed to give the key intermediate, 2-ketoglutaric acid. It may also be possible that the Gln could be effluxed and be transported out of the cells. We noticed that in comparison with [<sup>18</sup>F]4-FGln, **1** (2*S*,4*R*), [<sup>18</sup>F]4-FGln, **2** (2*S*,4*S*) or

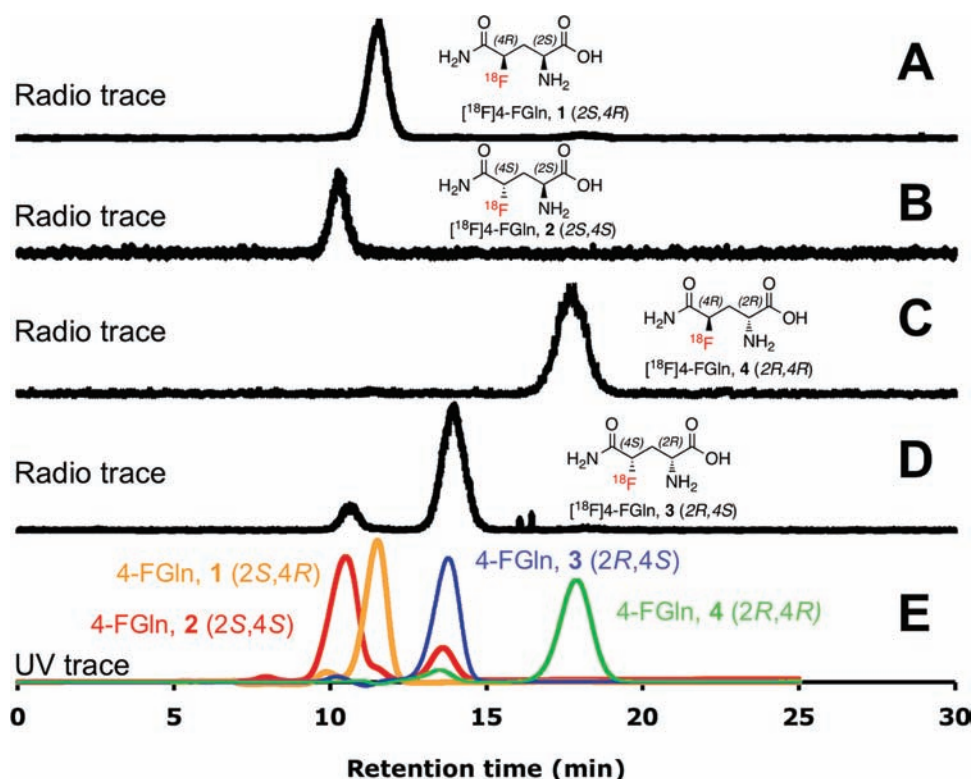
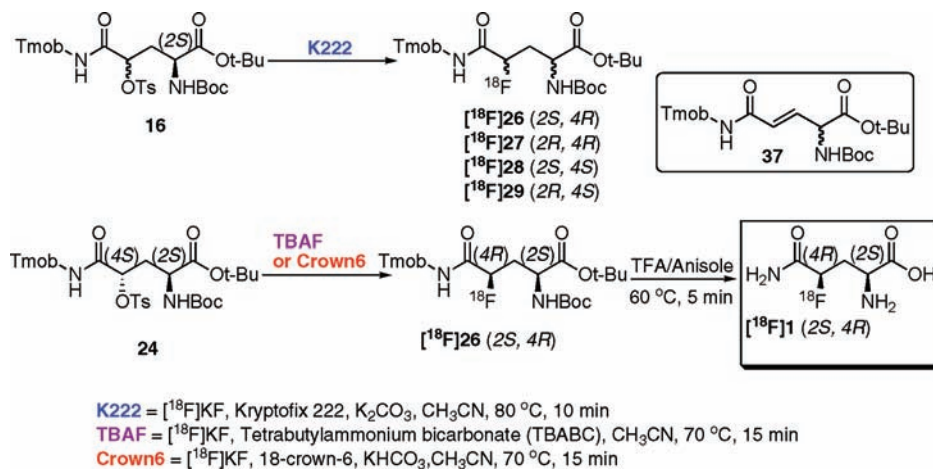


**Figure 6.** HPLC profiles of all four  $^{18}\text{F}$  labeled 4-FGln and the “cold” standards. Stationary phase: Chiral Chirex3126 (D-penicillamine) ( $150 \times 4.6$  mm); Mobile phase: 1 mM  $\text{CuSO}_4$ , 1 mL/min,  $10^\circ\text{C}$ . Traces A–D are the radio traces of the four  $^{18}\text{F}$  labeled isomers of 4-FGln; trace E is the UV spectra of the “cold” compounds 1, 2, 3, and 4 under identical HPLC conditions.

**Scheme 7. Exploration of Radio-Fluorination Reaction: Preparation of  $^{18}\text{F}$  1**



its metabolites may have a better ability to exit the 9L cells (Figure 8). We do not know if this is directly related to the transporter on the membrane or due to other metabolic processes. Preliminary metabolic studies of the cell uptake of the two L-Gln analogues,  $^{18}\text{F}$  1 (2S,4R) and  $^{18}\text{F}$  2 (2S,4S) suggested that the glutamines were taken up in the 9L cells by glutamine transporters<sup>70</sup> and predominantly converted to the corresponding  $^{18}\text{F}$  4-fluoro-glutamic acid (>60% at 30 min, 1 and 2 h after incubation) (data not shown). The most likely enzyme responsible would be L-glutaminase.<sup>19</sup> More detailed studies will be needed to explore the mechanisms responsible

for intracellular metabolism and trapping inside the cells. Such studies will be very important if these tracers are to be used for *in vivo* PET imaging of tumor growth.

Using SF188-Bcl-x<sub>L</sub> cells (derived from human glioblastoma cells), it was demonstrated that, as part of reprogramming of cellular metabolism, the cells showed glutamine addiction (Glutaminolysis).<sup>15,71</sup> The results suggest that the transcriptional regulatory properties of the oncogene Myc coordinate the expression of genes necessary for cells to engage in glutamine catabolism for protein and nucleotide biosynthesis. Myc-dependent glutaminolysis

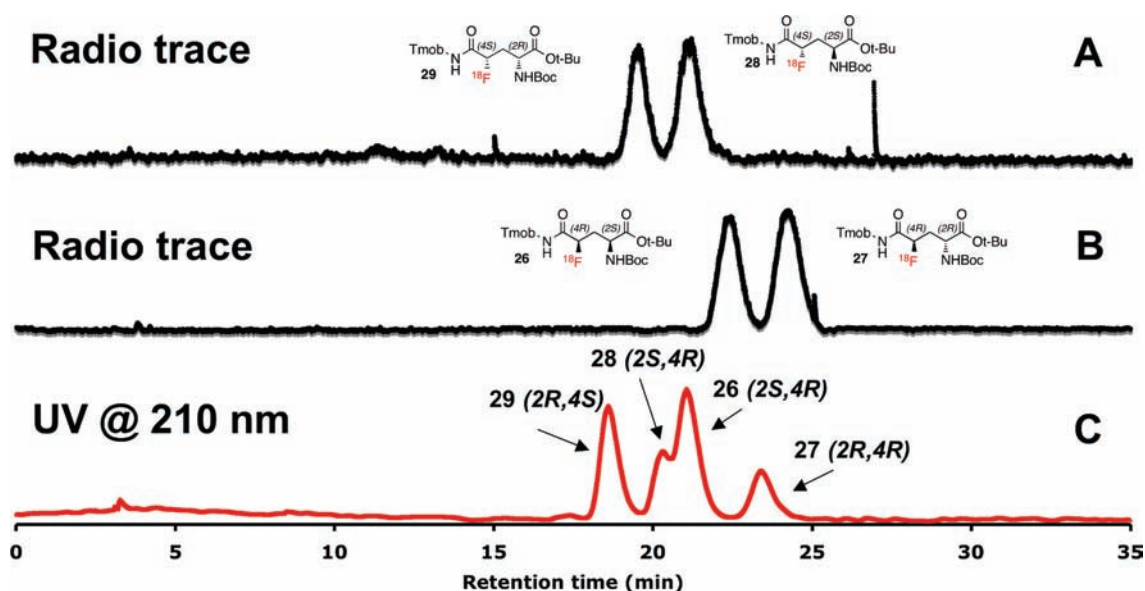
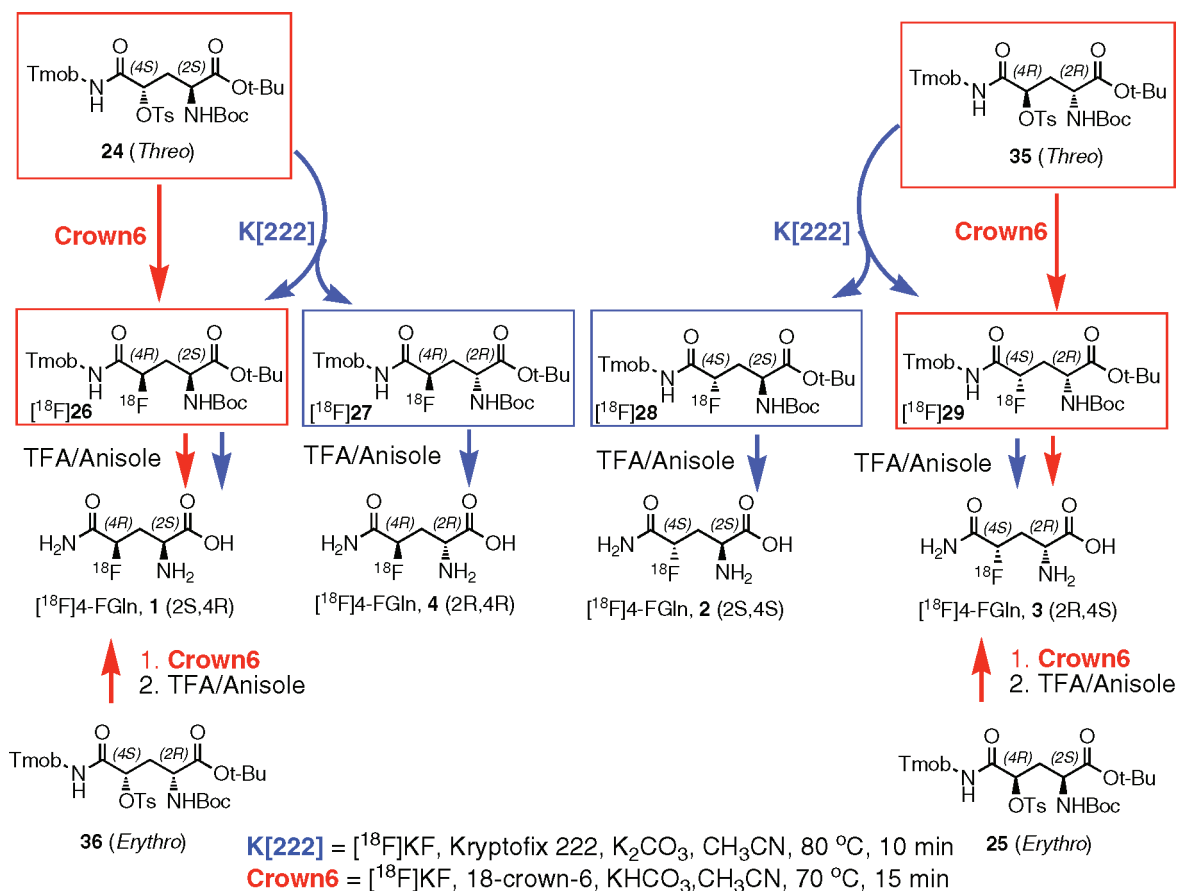


**Figure 7.** HPLC profiles of radio labeled intermediates from precursors 35 and 24 under  $K[222]/K_2CO_3$  conditions (traces A and B) with “cold” 4-FGln derivatives, 26, 27, 28, and 29 as reference (trace C). HPLC conditions, Chiralpak OD column; mobile phase, hexanes/EtOH 98.5/1.5; flow rate, 1.2 mL/min.

**Scheme 8.** Exploration of Radio-Fluorination Reaction: Preparation of All Four Isomers:  $[^{18}F]1$ ,  $[^{18}F]2$ ,  $[^{18}F]3$ , and  $[^{18}F]4$



redirected mitochondrial metabolism to depend on glutamine catabolism to sustain cellular viability and TCA cycle leading to the production of oxaloacetate (anaplerosis). The ability of

Myc-expressing SF188-Bcl-x<sub>L</sub> cells to promote glutaminolysis does not depend on concomitant activation of PI3K/Akt/mTOR pathway, which activates “aerobic glycolysis” (Warburg effect).



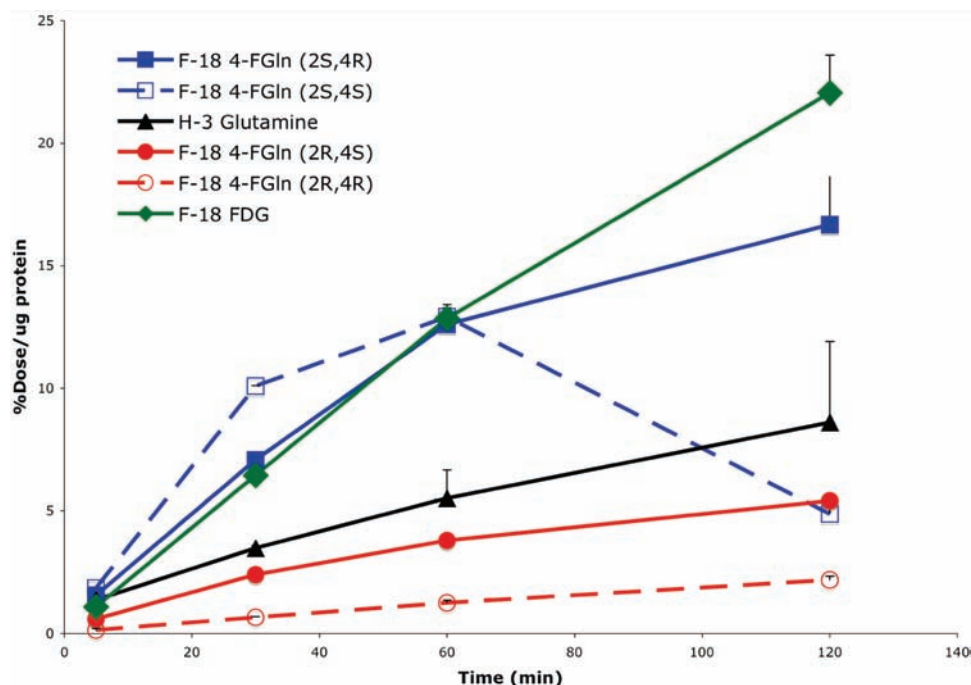
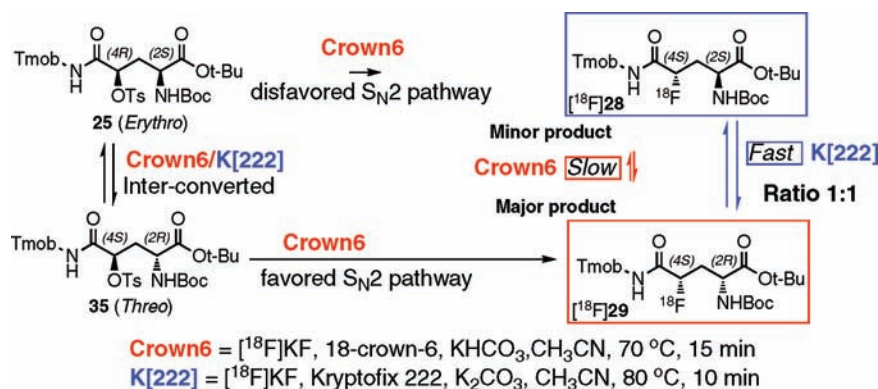


**Figure 8.** Cell uptake study results of all four [ $^{18}\text{F}$ ]4-FGln isomers ([ $^{18}\text{F}$ ]1, [ $^{18}\text{F}$ ]2, [ $^{18}\text{F}$ ]3, [ $^{18}\text{F}$ ]4), H-3 labeled Gln, and [ $^{18}\text{F}$ ]FDG. All radiotracers were evaluated in the 9L tumor cell line.

**Scheme 9.** Tentative Explanation for the Formation of [ $^{18}\text{F}$ ]29 as a Major Product with Tosylate 25 (2S,4R) as the Precursor in the Presence of 18-Crown-6 and  $\text{KHCO}_3$  and the Formation of a 1 to 1 Ratio of [ $^{18}\text{F}$ ]28 and [ $^{18}\text{F}$ ]29 under the  $\text{K}[222]/\text{K}_2\text{CO}_3$  Conditions



The stimulation of mitochondrial glutamine metabolism resulted in reduced glucose carbon entering the TCA cycle and a decreased contribution of glucose to the mitochondrial-dependent synthesis of phospholipids. As such, SF188-Bcl- $x_L$  tumor cells will serve as a suitable model for testing the glutamine uptake and retention from which an estimation of glutamine utilization may be feasible.

To demonstrate that the transformed SF188-Bcl- $x_L$  tumor cells can preferentially take up glutamine, we have studied the cell uptake of  $^{18}\text{F}$ -FDG and  $^3\text{H}$ -glutamine as tracers simultaneously in phosphate buffered saline (PBS). Results presented in Figure 9 demonstrated a clear and prominent uptake of  $^3\text{H}$ -glutamine in these cells (10–12% dose/100  $\mu\text{g}$  of protein after 60 min incubation). The uptake of glutamine and FDG in the cells suggest that the tumor cells utilize both glucose ( $^{18}\text{F}$ -FDG) and  $^3\text{H}$ -glutamine. As demonstrated

previously, the SF188-Bcl- $x_L$  tumor cells use glutamine and glucose as a source of metabolic energy.<sup>15,71</sup> Notably, the uptake of glutamine (10% dose/100  $\mu\text{g}$  of protein) into the SF188-Bcl- $x_L$  tumor cells was twice as high as that of  $^{18}\text{F}$ -FDG (5% dose/100  $\mu\text{g}$  of protein) after 60 min incubation, suggesting that they are undergoing “glutaminolysis” (Figure 9).

Under the same *in vitro* incubation condition, the uptake of two [ $^{18}\text{F}$ ]4-FGln, 1 (2S,4R), and 2 (2S,4S), into SF188-Bcl- $x_L$  cells demonstrated a dramatically higher uptake than that of  $^3\text{H}$ -glutamine and  $^{18}\text{F}$ -FDG (Figure 9). It is noted that [ $^{18}\text{F}$ ]4-FGln, 1 displayed an uptake of 22% dose/100  $\mu\text{g}$  of protein at 60 min, while the other isomer, [ $^{18}\text{F}$ ]4-FGln, 2 (2S,4S), showed a faster kinetics, and the uptake peaked (21% dose/100  $\mu\text{g}$  of protein) at 30 min after incubation. Preliminary metabolism analysis indicated

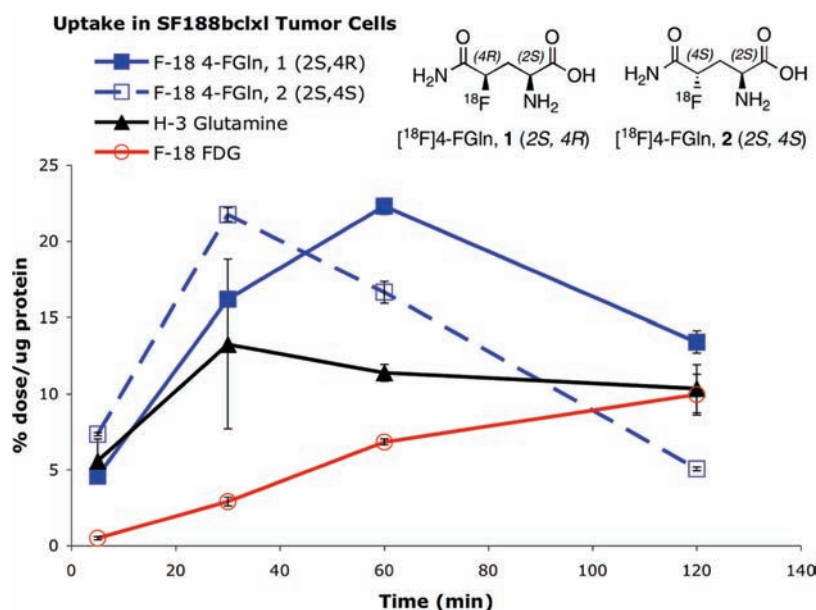


**Figure 9.** Results of uptake of two  $[^{18}\text{F}]4\text{-FGln, 1 (2S,4R)}$ , and  $2 (2S,4S)$ , into SF188-Bcl- $x_L$  tumor cells: ( $[^{18}\text{F}]1$  in solid blue), ( $[^{18}\text{F}]2$  in dashed blue),  $^3\text{H-Gln}$  (in black), and  $[^{18}\text{F}]FDG$  (in red).

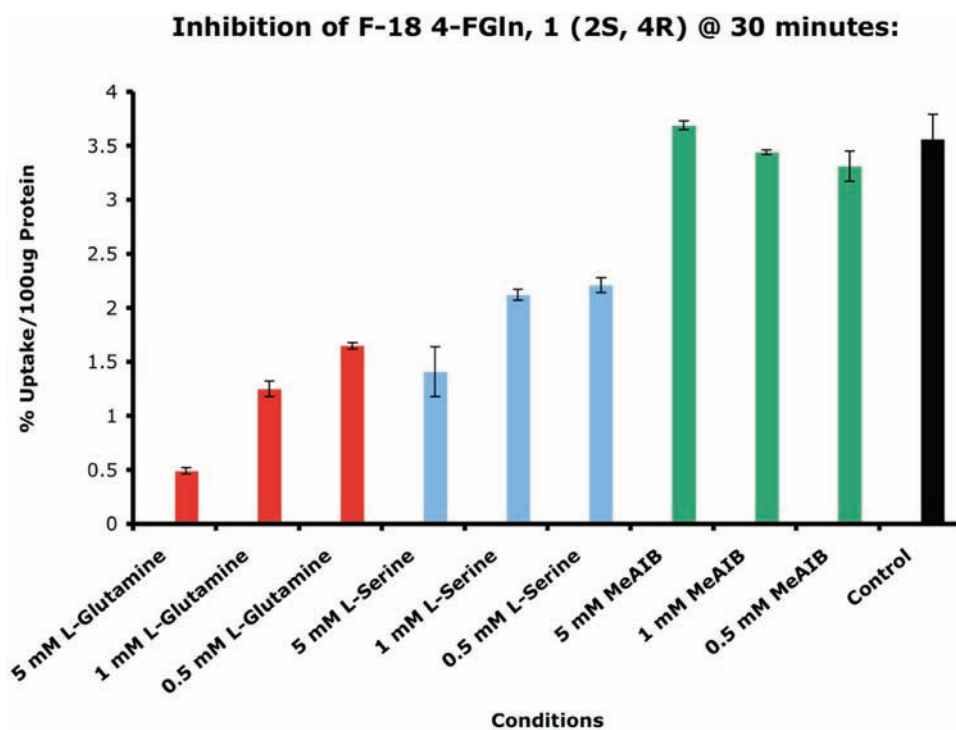


**Figure 10.** *In vitro* cell uptake inhibition studies of  $[^{18}\text{F}]4\text{-FGln, 1 (2S,4R)}$  conducted in 9L cells.

that the  $[^{18}\text{F}]4\text{-FGln, 1 (2S,4R)}$  and  $2 (2S,4S)$ , both converted to the corresponding glutamic acids as found in the 9L cells, but  $[^{18}\text{F}]4\text{-FGln, 2 (2S,4S)}$  showed a higher defluorination (data not shown). The results suggest that the  $[^{18}\text{F}]4\text{-FGln, 1 (2S,4R)}$  and  $2 (2S,4S)$  may be better than  $^3\text{H-glutamine}$  with a higher propensity as the alternative energy source. The differences in cell uptake between the 4S versus 4R isomer of  $[^{18}\text{F}]4\text{-FGln}$  were highly significant. Despite some previous reports on 4-FGln, such disparities on biological properties between stereoisomers have never

been predicted or mentioned before. The synthesis and radiolabeling method reported in this paper will make it possible to investigate the novel observation further. The *in vitro* tumor cell uptake studies suggest that the  $[^{18}\text{F}]4\text{-FGln, 1 (2S,4R)}$  will be a preferred isomer for *in vivo* imaging. Detailed *in vivo* imaging studies are warranted to fully characterize the relationship of tumor uptake and glutaminolysis.

Among all the  $[^{18}\text{F}]4\text{-FGln}$  isomers,  $[^{18}\text{F}]4\text{-FGln, 1 (2S,4R)}$  displayed the highest uptake by the 9L tumor cells. Because of

this observation, we only used this [ $^{18}\text{F}$ ]4-FGln tracer in our further investigations. *In vitro* cell uptake inhibition studies were conducted in 9L cells in order to test the specificity of this radiotracer (Figure 10). Two natural amino acids, L-Gln and L-serine, served as the positive control inhibitors for the Gln transporters. L-Gln inhibits the system N transporter and L-serine inhibits the ASC transporter. Three different concentrations were tested for each inhibitor ranging from 0.5 to 5 mM. After 30 min of coinubation of L-Gln and [ $^{18}\text{F}$ ]4-FGln, **1** (2S,4R), the system N transporter was clearly inhibited. The results showed nearly 90% inhibition (0.49% dose/100  $\mu\text{g}$  protein inhibited vs control 3.56% dose/100  $\mu\text{g}$  protein). L-Serine also showed considerable inhibition (1.41% inhibited vs control 3.56% dose/100  $\mu\text{g}$  protein) of the ASC transporter. MeAIB, which inhibits the system A transporter, served as the negative control. At a concentration of 5 mM, there was little or no effect on the system A transport system (3.69% inhibited vs control 3.56% dose/100  $\mu\text{g}$  protein). The results clearly demonstrate a dose-dependent response to L-Gln and L-serine, with MeAIB showing no inhibition of the system A transport system.

Additional biological evaluation of the most promising Gln analogue [ $^{18}\text{F}$ ]4-FGln, **1** (2S,4R) isomer in normal and tumor bearing mice by PET imaging and biodistribution demonstrated that the Gln tracer indeed localized in the tumor tissue *in vivo* (data not shown). These results, which will be reported in other publications, further support our findings that the new L-Gln analogue, [ $^{18}\text{F}$ ]4-FGln, **1** (2S,4R), is metabolized by tumor tissue.

## CONCLUSIONS

In summary, a new synthetic pathway to 4-FGln derivatives was developed. The synthesis of all four optically pure 4-FGln was accomplished using a Passerini three-component reaction and "neutralized" TASF nucleophilic fluorination reaction as key steps. In addition, tosylates **24**, **25**, **35**, and **36**, which are suitable precursors for  $^{18}\text{F}$  radio-fluorination reactions, were synthesized on grams scale. It is reasonable to postulate that this synthetic method could be used to synthesize various functional group substituted (at the 4-position) and optically enriched Gln or glutamic acid analogues, since fluoro-substituted functionalization, one of the hardest functionalization processes, has been performed. In addition, we successfully accomplished the syntheses of four stereoisomeric  $^{18}\text{F}$  4-FGlns, [ $^{18}\text{F}$ ]**1**, [ $^{18}\text{F}$ ]**2**, [ $^{18}\text{F}$ ]**3**, and [ $^{18}\text{F}$ ]**4**. *In vitro* cell uptake studies (9L tumor cells) suggest that uptake is highly specific for two of the L-Gln analogues, [ $^{18}\text{F}$ ]**1** (2S,4R) and [ $^{18}\text{F}$ ]**2** (2S,4S), and it is likely associated with the native L-Gln transporters. Between them, [ $^{18}\text{F}$ ]**1** (2S,4R) was selected as the leading probe for further biological evaluation. We hope that the successful development of this new metabolic probe for the detection of glutaminolysis will contribute to the advancement of cancer diagnosis and therapy.

## ASSOCIATED CONTENT

**S** Supporting Information. Full experimental procedures and data,  $^1\text{H}/^{13}\text{C}$ NMR spectra of new compounds, HPLC profiles and reported X-ray structural data. This material is available free of charge via the Internet at <http://pubs.acs.org>.

## AUTHOR INFORMATION

### Corresponding Author

wenchao@mail.med.upenn.edu; kungfh@sunmac.spect.upenn.edu

## ACKNOWLEDGMENT

We thank Stand Up 2 Cancer (SU2C) for financial support. Authors thank Dr. Chaitanya Divgi for helpful discussions. Authors also want to thank Dr. Carita Huang for her editorial assistance.

## REFERENCES

- (1) Jaeckel, C.; Koksche, B. *Eur. J. Org. Chem.* **2005**, 4483.
- (2) Meng, H.; Kalsani, V.; Kumar, K. *ACS Symp. Ser.* **2007**, 949, 487.
- (3) Jaeckel, C.; Salwiczek, M.; Koksche, B. *Angew. Chem., Int. Ed.* **2006**, 45, 4198.
- (4) Meng, H.; Kumar, K. *J. Am. Chem. Soc.* **2007**, 129, 15615.
- (5) Zheng, H.; Comeforo, K.; Gao, J. *J. Am. Chem. Soc.* **2009**, 131, 18.
- (6) Chiu, H.-P.; Kokona, B.; Fairman, R.; Cheng, R. P. *J. Am. Chem. Soc.* **2009**, 131, 13192.
- (7) O'Hagan, D. *Chem. Soc. Rev.* **2008**, 37, 308.
- (8) Purser, S.; Moore, P. R.; Swallow, S.; Gouverneur, V. *Chem. Soc. Rev.* **2008**, 37, 320.
- (9) Mercer, J. R. *J. Pharm. Pharm. Sci.* **2007**, 10, 180.
- (10) McConathy, J.; Goodman Mark, M. *Cancer Metastasis Rev.* **2008**, 27, 555.
- (11) Schuster, D. M.; Votaw, J. R.; Nieh, P. T.; Yu, W.; Nye, J. A.; Master, V.; Bowman, F. D.; Issa, M. M.; Goodman, M. M. *J. Nucl. Med.* **2007**, 48, 56.
- (12) Laverman, P.; Boerman, O. C.; Corstens, F. H. M.; Oyen, W. J. G. *Eur. J. Nucl. Med. Mol. Imaging* **2002**, 29, 681.
- (13) Jager, P. L.; Vaalburg, W.; Pruim, J.; de Vries, E. G.; Langen, K. J.; Piers, D. A. *J. Nucl. Med.* **2001**, 42, 432.
- (14) Plathow, C.; Weber, W. A. *J. Nucl. Med.* **2008**, 49 (Suppl. 2), 43S.
- (15) Wise, D. R.; DeBerardinis, R. J.; Mancuso, A.; Sayed, N.; Zhang, X.-Y.; Pfeiffer, H. K.; Nissim, I.; Daikhin, E.; Yudkoff, M.; McMahon, S. B.; Thompson, C. B. *Proc. Natl. Acad. Sci. U.S.A.* **2008**, 105, 18782.
- (16) DeBerardinis, R. J.; Lum, J. J.; Hatzivassiliou, G.; Thompson, C. B. *Cell Metab.* **2008**, 7, 11.
- (17) Vander Heiden, M. G.; Cantley, L. C.; Thompson, C. B. *Science* **2009**, 324, 1029.
- (18) Thompson, C. B. *N. Eng. J. Med.* **2009**, 360, 813.
- (19) Gao, P.; Tchernyshyov, I.; Chang, T. C.; Lee, Y. S.; Kita, K.; Ochi, T.; Zeller, K. I.; De Marzo, A. M.; Van Eyk, J. E.; Mendell, J. T.; Dang, C. V. *Nature* **2009**, 458, 762.
- (20) Dang, C. V. *Cancer Res.* **2010**, 70, 859.
- (21) Qiu, X.-L.; Meng, W.-D.; Qing, F.-L. *Tetrahedron* **2004**, 60, 6711.
- (22) Smits, R.; Cadicamo, C. D.; Burger, K.; Koksche, B. *Chem. Soc. Rev.* **2008**, 37, 1727.
- (23) Pigza, J. A.; Quach, T.; Molinski, T. F. *J. Org. Chem.* **2009**, 74, 5510.
- (24) Hu, Z.; Han, W. *Tetrahedron Lett.* **2008**, 49, 901.
- (25) Padmakshan, D.; Bennett, S. A.; Otting, G.; Easton, C. J. *Synlett* **2007**, 1083.
- (26) Li, G.; van der Donk, W. A. *Org. Lett.* **2007**, 9, 41.
- (27) Suzuki, A.; Mae, M.; Amii, H.; Uneyama, K. *J. Org. Chem.* **2004**, 69, 5132.
- (28) Hoveyda, H. R.; Pinault, J.-F. *Org. Lett.* **2006**, 8, 5849.
- (29) Chorghade, M. S.; Mohapatra, D. K.; Sahoo, G.; Gurjar, M. K.; Mandlecha, M. V.; Bhoite, N.; Moghe, S.; Raines, R. T. *J. Fluorine Chem.* **2008**, 129, 781.
- (30) Charrier, J.-D.; Hadfield, D. S.; Hitchcock, P. B.; Young, D. W. *Org. Biomol. Chem.* **2004**, 2, 797.
- (31) Charrier, J.-D.; Hadfield, D. S.; Hitchcock, P. B.; Young, D. W. *Org. Biomol. Chem.* **2004**, 2, 474.
- (32) Charrier, J.-D.; Hitchcock, P. B.; Young, D. W. *Org. Biomol. Chem.* **2004**, 2, 1310.
- (33) Qiu, X.-L.; Meng, W.-D.; Qing, F.-L. *Tetrahedron* **2004**, 60, 5201.
- (34) Yajima, T.; Nagano, H. *Org. Lett.* **2007**, 9, 2513.
- (35) Mykhailiuk, P. K.; Afonin, S.; Chernega, A. N.; Rusanov, E. B.; Platonov, M. O.; Dubinina, G. G.; Berditsch, M.; Ulrich, A. S.; Komarov, I. V. *Angew. Chem., Int. Ed.* **2006**, 45, 5659.

- (36) Mykhailiuk, P. K.; Afonin, S.; Palamarchuk, G. V.; Shishkin, O. V.; Ulrich, A. S.; Komarov, I. V. *Angew. Chem., Int. Ed.* **2008**, *47*, 5765.
- (37) Shendage, D. M.; Froehlich, R.; Bergander, K.; Haufe, G. *Eur. J. Org. Chem.* **2005**, 719.
- (38) Dave, R.; Badet, B.; Meffre, P. *Amino Acids* **2003**, *24*, 245.
- (39) Tolmana, V.; Sedmera, P. *J. Fluorine Chem.* **2000**, *101*, 5.
- (40) (a) Dinkelborg, L.; Friebe, M.; Krasikowa, R. N.; Belokon, Y.; Kuznetsova, O. F.; Graham, K.; Lehmann, L.; Berndt, M. EP 2007/009518, WO/2008/052788, 2008. (b) Krasikova, R. N.; Kuznetsova, O. F.; Fedorova, O. S.; Belokon, Y. N.; Maleev, V. L.; Mu, L.; Ametamey, S.; Schubiger, P. A.; Friebe, M.; Berndt, M.; Koglin, N.; Mueller, A.; Graham, K.; Lehmann, L.; Dinkelborg, L. M. *J. Med. Chem.* **2010**, DOI: 10.1021/jm101068q. (c) Friebe, M.; Schmitt-willich, H.; Berndt, M.; Dinkelborg, L.; Koglin, N.; Graham, K. U.S. Patent Application 20100290991-A1.
- (41) Domling, A. *Chem. Rev.* **2006**, *106*, 17.
- (42) Hulme, C.; Gore, V. *Curr. Med. Chem.* **2003**, *10*, 51.
- (43) Hudson, D. USP 4 935 536, 1990.
- (44) Weygand, F.; Steglich, W.; Bjarnason, J. *Chem. Ber* **1968**, *101*, 3642.
- (45) Pietta, P. G.; Biondi, P. A.; Brenna, O. *J. Org. Chem.* **1976**, *41*, 703.
- (46) Armstrong, A.; Brackenridge, I.; Jackson, R. F. W.; Kirk, J. M. *Tetrahedron Lett.* **1988**, *29*, 2483.
- (47) Bergmeier, S. C.; Cobas, A. A.; Rapoport, H. *J. Org. Chem.* **1993**, *58*, 2369.
- (48) Adlington, R. M.; Baldwin, J. E.; Catterick, D.; Pritchard, G. J. *J. Chem. Soc., Perkin Trans. 1* **1999**, 855.
- (49) Ramsamy, K.; Olsen, R. K.; Emery, T. *Synthesis* **1982**, 42.
- (50) Dess, D. B.; Martin, J. C. *J. Org. Chem.* **1983**, *48*, 4155.
- (51) Werner, R. M.; Shokek, O.; Davis, J. T. *J. Org. Chem.* **1997**, *62*, 8243.
- (52) Wernic, D.; DiMaio, J.; Adams, J. *J. Org. Chem.* **1989**, *54*, 4224.
- (53) Pigge, F. C.; Coniglio, J. J.; Fang, S. *Organometallics* **2002**, *21*, 4505.
- (54) Costa, S. P. G.; Maia, H. L. S.; Pereira-Lima, S. M. M. A. *Org. Biomol. Chem.* **2003**, *1*, 1475.
- (55) Masaki, M.; Kitahara, T.; Kurita, H.; Ohta, M. *J. Am. Chem. Soc.* **1968**, *90*, 4508.
- (56) Naruto, M.; Ohno, K.; Naruse, N.; Takeuchi, H. *Tetrahedron Lett.* **1979**, 251.
- (57) Middleton, W. J. *J. Org. Chem.* **1975**, *40*, 574.
- (58) Konas, D. W.; Coward, J. K. *J. Org. Chem.* **2001**, *66*, 8831.
- (59) Pilcher, A. S.; Ammon, H. L.; DeShong, P. *J. Am. Chem. Soc.* **1995**, *117*, 5166.
- (60) Gingras, M. *Tetrahedron Lett.* **1991**, *32*, 7381.
- (61) Chang, C.-Y.; Yang, T.-K. *Tetrahedron: Asymmetry* **2003**, *14*, 2239.
- (62) Yin, J.; Zarkowsky, D. S.; Thomas, D. W.; Zhao, M. M.; Huffman, M. A. *Org. Lett.* **2004**, *6*, 1465.
- (63) RajanBabu, T. V.; Middleton, W. J.; Tortorelli, V. J.; *e-EROS Encyclopedia of Reagents for Organic Synthesis*; John Wiley & Sons: New York, 2001
- (64) Greene, T. W.; Wuts, P. G. M., 3rd ed.; John Wiley & Sons, Inc.: New York City, 1999.
- (65) Krasnov, V. P.; Koroleva, M. A. *Russ. Chem. Bull.* **1995**, 631.
- (66) Krasnov, V. P.; Koroleva, M. A.; Evstigneeva, N. G.; Nizova, I. A. *Russ. Chem. Bull.* **1995**, 635.
- (67) Kim, D. W.; Ahn, D. S.; Oh, Y. H.; Lee, S.; Kil, H. S.; Oh, S. J.; Lee, S. J.; Kim, J. S.; Ryu, J. S.; Moon, D. H.; Chi, D. Y. *J. Am. Chem. Soc.* **2006**, *128*, 16394.
- (68) Yu, W.; Williams, L.; Camp, V.; Olson, J.; Goodman, M. *Bioorg. Med. Chem. Lett.* **2010**, *20*, 2140.
- (69) Wang, L.; Qu, W.; Lieberman, B.; Ploessl, K.; Kung, H. *Bioorg. Med. Chem. Lett.* **2010**, *20*, 3482.
- (70) McGivan, J. D.; Bungard, C. I. *Front. Biosci.* **2007**, *12*, 874.
- (71) DeBerardinis, R. J.; Mancuso, A.; Daikhin, E.; Nissim, I.; Yudkoff, M.; Wehrli, S.; Thompson, C. B. *Proc. Natl. Acad. Sci. U.S.A.* **2007**, *104*, 19345.